THE ASTROPHYSICAL JOURNAL, 292:348–356, 1985 May 15

THE GRAVITATIONAL LENS AS AN ASTRONOMICAL DIAGNOSTIC

WILLIAM C. SASLAW
Department of Astronomy, University of Virginia; Institute of Astronomy, Cambridge, England; and National Radio Astronomy Observatory,[1] Charlottesville, Virginia

D. NARASIMHA
Tata Institute of Fundamental Research, Bombay; Department of Physics, University of Calgary, Alberta, Canada

AND

S. M. CHITRE
Tata Institute of Fundamental Research, Bombay
Received 1984 August 27; accepted 1984 November 21

ABSTRACT

We examine how a point gravitational lens images a diffuse background source, and show that under a wide range of circumstances the image contains a "gravity ring." The chief criterion for producing this phenomenon is that the angular scale of brightness variation in the source be smaller than the angular radius of the cone of inversion of the image.

The observation of gravity rings, which should soon become resolvable with very long baseline radio interferometry, would provide a useful astronomical diagnostic. It would give an independent (or unique) estimate of fundamental quantities such as the mass or distance of the deflector star and the distance of the source. We describe a variety of astronomical examples, such as nebulae and pulsars, where the phenomenon may be especially useful.

Subject headings: gravitation — interferometry — pulsars

I. INTRODUCTION

We predict that in the next few years, when very long baseline interferometry (VLBI) provides sensitive detailed high-resolution maps, it will reveal a new type of astronomical image: the "gravity ring." This phenomenon will make possible a new technique for determining such properties as masses of pulsars, the mass spectrum of stars in clusters (from binaries to globular clusters), distances to galactic gas clouds (including planetary nebulae and supernova remnants), and information about H II regions with even higher resolution than the VLB array would nominally provide.

Gravity rings are an overlooked aspect of a classical subject: gravitational lenses. The reason that the importance of gravity rings has been overlooked is probably two fold. First, their observation requires high resolution and mapping ability slightly beyond the present state of the art. Second, the emphasis in gravitational lens theory originally centered around the imaging of a point source by a point lens and, more recently, around the imaging of a point source (quasar) by an extended lens (galaxy or cluster of galaxies). Gravity rings, however, are most important for the *imaging of an extended source by a point lens*. Moreover, the effect works best within our own Galaxy.

Gravitational lenses have been recognized since Einstein (1936), following Mandl's suggestion, calculated the gravitational focusing of a distant star's light by a foreground star nearly aligned with the observer. He concluded that the chance of observing such a phenomenon was not very high. Zwicky (1937) then applied the idea to galaxies, suggesting that a nearby galaxy along the line of sight could create a double image of a distant background galaxy, or a ring in the case of perfect alignment, and that this might provide a method for determining galaxy masses. In the mid 1960s, Barnothy (1965) revived the subject by suggesting that quasars were compact sources such as Seyfert nuclei, whose luminosity is gravitationally magnified by a massive object en route acting as a lens. The long-expected discovery of a gravitational lens system came when Walsh, Carswell, and Weymann (1979) found two quasars separated by 6″.15 with almost identical redshifts of 1.41. Since then, four more cases have been reported as likely candidates for gravitational lenses. Gott (1981) has suggested using the gravitational lensing of quasars as a way to detect low-mass stars in galaxy halos.

The earlier analyses of lenses concerned light from a background point source being deflected by a point mass (M) at impact parameter b through an angle $4GM/c^2b$ radians. Stockton's (1980) discovery of a giant elliptical member of a cluster of galaxies at a redshift 0.39 along the line of sight to the double quasar of Walsh *et al.* prompted the construction of detailed models to reproduce this configuration (cf. Young *et al.* 1981; Narasimha, Subramanian, and Chitre 1982). These models examined extended (distributed) lenses for imaging the background quasar, which was treated as a point source. The mathematical formalism of Bourassa and Kantowski (1975) is particularly useful for these distributed lenses.

In the present paper, however, we shall be concerned with imaging of extended background sources by a point mass. The gravitational lens effect for diffuse sources has been considered by Liebes (1964), Refsdal (1964), and Bontz (1979), who have discussed the luminosity enhancement of the background source. Here our interest is in the shape of the image, especially in the conditions needed to produce gravity rings which can be detected with very long baseline interferometry, and in what can be learned from such rings.

Section II gives a brief review of the simple properties of gravitational lenses which are basic to our discussion. In § III

[1] The National Radio Astronomy Observatory is operated by Associated Universities, Inc., under contract with the National Science Foundation.

we derive the fundamental criterion for the appearance of gravity rings. This is just that the angular scale length of intensity variation in the extended background source should be smaller than the angular "cone of inversion" (scale of gravitational influence) of the point-mass deflector. Section IV shows examples of gravity rings produced for different backgrounds using both numerical computations and a gravitational analog lens made of Plexiglas. Section V discusses representative conditions in which gravity rings can be a useful astronomical diagnostic.

II. BASIC PROPERTIES OF POINT GRAVITATIONAL LENSES

In this section we review those aspects of gravitational lenses relevant to our analysis, in order to establish our notation. Our approach is similar to that of Liebes (1964). We make a slight generalization to vector form which enables us to calculate two-dimensional images more readily and thus extend the point source.

We begin by considering a source point located at S whose light rays are deflected by a point mass at D and then seen by an observer at O, as Figure 1 illustrates. We project the source and image positions onto a plane passing through the deflector and orthogonal to the line of sight to the source. The distances of these source and image positions from D are $\boldsymbol{r}$ and $\boldsymbol{r}_I$ respectively. We denote the observer-deflector distance by l_{OD}, the deflector-source distance by l_{DS}, and the observer-source distance by l_{OS}. Moreover, α is the angular displacement of the source from the deflector. For general positions of the source, deflector, and observer, there will be two possible light paths, SPO and SQO, from each point on the source to the observer. These will produce images I_1 and I_2 which appear to have

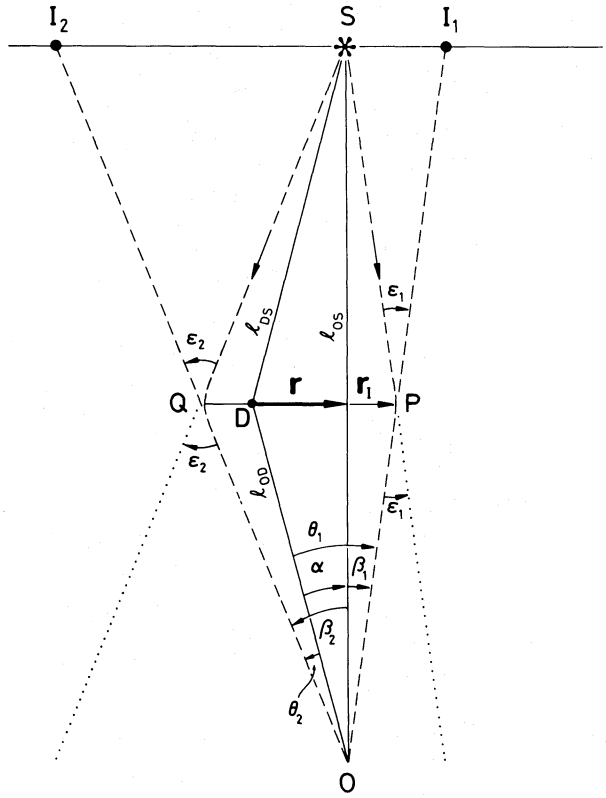

FIG. 1.—The geometry of a simple gravitational deflector

angular displacements θ_1 and θ_2 from the deflector. The bending angle is

$$\epsilon = \frac{4GM}{c^2|\boldsymbol{r}_I|} \tag{1}$$

for each ray $\boldsymbol{r}_1$ and $\boldsymbol{r}_2$. The observer sees the image I_1 from a ray which remains closer to the original source but appears farther from the deflector, since the bending angle varies inversely as the ray's impact parameter. This shows us that the lens will invert images.

To determine the important geometrical relations in a simple way, we note that since the deflections are small, the distance $SI_1 = \epsilon_1 l_{DS} = \beta_1 l_{OS}$ to a very good approximation. Moreover, $\theta_1 = r_I/l_{OD}$. Multiply these two equations together and substituting equation (1) for ϵ_1, we may write the result as

$$\beta_1 = \frac{\epsilon_1 l_{DS} r_I}{\theta_1 l_{OS} l_{OD}} = \frac{\theta_0^2}{\theta_1}, \tag{2}$$

where

$$\theta_0^2 \equiv \frac{\mu}{l_{OD}^2}, \tag{3}$$

and

$$\mu \equiv \frac{4GM}{c^2}\frac{l_{OD} l_{DS}}{l_{OS}} \tag{4}$$

is the lens strength.

Similar analysis of the second image shows $\beta_2\theta_2 = \theta_0^2 = \beta_1\theta_1$. Since $\beta_2 \neq \beta_1$ and $\theta_2 \neq \theta_1$ by construction (except for perfect alignment), we obtain $\beta_1 = \theta_2$ and $\beta_2 = \theta_1$ from the geometry, and thus $\theta_1\theta_2 = \theta_0^2$. The angle θ_0 denotes what Liebes (1964), using a generally different notation, calls the "cone of inversion." The external image I_1 has $\theta_1 > \theta_0$ and thus appears outside the cone of inversion, while the internal image I_2 with $\theta_2 < \theta_0$ appears within the cone. For the exceptional case of perfect alignment, $\theta_1 = \theta_2$, and by symmetry the image must form a circle with radius θ_0 around the deflector.

To find the form of a simple image produced by many source points, we note from Figure 1 that $\theta_1 = \alpha + \beta_1$, and thus, again for small-angle deflections,

$$\boldsymbol{r}_I = \boldsymbol{r} + l_{OD}\beta_1 \frac{\boldsymbol{r}_I}{|\boldsymbol{r}_I^2|^{1/2}} = \boldsymbol{r} + \frac{\mu}{r_I^2}\boldsymbol{r}_I, \tag{5}$$

using equations (2) and (3). The scalar product of this result with $\boldsymbol{r}_I$ yields

$$r_I^2 - rr_I - \mu = 0, \tag{6}$$

whose two roots determine the positions r_1 and r_2 of the external and internal image points. Since angular coordinates are more directly observable, we divide equation (6) through by l_{OD}^2 to obtain

$$\theta^2 - \alpha\theta - \theta_0^2 = 0. \tag{7}$$

Note that the roots of this equation directly give the relations $\theta_1 - \theta_2 = \alpha$ and $\theta_1\theta_2 = \theta_0^2$. The angular separation between the two images is $(\alpha^2 + 4\theta_0^2)^{1/2}$, and the separation between the internal image and the deflector is $[(\alpha^2 + 4\theta_0^2)^{1/2} - \alpha]/2$.

The angular radius of the cone of inversion is thus one of the most important properties of the lens system. In handy units we may express it as

$$\theta_0 = 2.9\left(\frac{M}{M_\odot}\right)^{1/2}\left|\frac{l_{DS}}{l_{OD}\, l_{OS}}\right|_{\text{kpc}}^{1/2} \text{ milli-arcseconds}, \tag{8}$$

where distances are measured in kiloparsecs. To detect structure around the cone of inversion requires accurate mapping ability (good U-V plane coverage) as well as high resolution. Both should be well within the capability of proposed radio VLBI arrays.

III. THE CRITERION FOR GRAVITY RINGS

The image of an extended source will show structure around the angular radius of the cone of inversion only if the brightness of the source varies over its area. Since the surface brightness is invariant under imaging by a gravitational lens (the increased intensity of an image being caused by its increased surface area), no effect will be seen when a uniformly bright source subtends an angle greater than the cone of inversion. Moreover, any effects will be obscured if the cone of inversion is covered by the deflector. A star of 10^{11} cm radius has an angular diameter of 6.6×10^{-3} milli-arcseconds at 1 kpc, so this second criterion will be satisfied easily for many galactic configurations of stars and interstellar clouds. Neutron stars satisfy it even more easily. We therefore turn to the more interesting criterion of brightness contrast.

The effect of a point lens on an extended source is to image one part of the source onto the area which would have formed another part of the source. This displaces the image contours with respect to the corresponding source contours. The amount of angular displacement, $\Delta\theta = \theta - \alpha$, follows from equation (2):

$$\Delta\theta = \frac{\theta_0^2}{\theta} . \tag{9}$$

Provided that we are not dealing with a local brightness maximum or minimum of the source, we may expand its brightness distribution $B(\theta)$ in a Taylor series, retaining just the first-order term for simplicity:

$$B = B_0\left(1 + \frac{\theta}{\Omega}\right), \tag{10}$$

where Ω may be regarded as an angular scale length. The brightness contrast at θ between the background source and the image is then given by

$$\Delta B \approx \frac{dB}{d\theta}\,\Delta\theta = B_0\,\frac{\theta_0^2}{\Omega\theta} . \tag{11}$$

This analysis assumes, of course, that the resolution, δ, is smaller than $\Delta\theta$.

The maximum brightness contrast of a contour will depend on whether it is exterior or interior to the cone of inversion at angular radius θ_0. Exterior contours are more readily observed, since they may be seen with lower resolution telescopes. The minimum value of θ for exterior contours is θ_0, and consequently, from equation (11), their maximum brightness contrast will be $B_0\,\theta_0/\Omega$. Therefore the lens produces a large fractional change in the contrast of the exterior image contours if

$$\frac{\theta_0}{\Omega} \gtrsim 1 . \tag{12}$$

This is the basic criterion for the production of easily observable gravity rings. The angular scale of source intensity variation must be small compared with the angular radius of the cone of inversion.

The analysis of interior contours is a bit more intricate. Although these are not as readily observed, they have interesting properties which we report briefly here. The essential difference between interior and exterior contours arises because, as Figure 1 indicates, interior image rays come from parts of the source which are very strongly deflected. Such rays may come from quite different areas of the source, with a wide range of surface brightness, all of which are deflected into the small angular area of the cone of inversion. Moreover, the magnification (or reduction) of an elemental surface area of the source may be considerable when it is mapped into the cone of inversion. As a result, the surface brightness of the interior image will vary strongly with angular position, and its apparent intensity will depend significantly on the resolution of the observation.

To examine the interior image in more detail, we consider some region of the image plane enclosed by a typical contour. The excess of flux from this region over the background may be estimated as follows: We move to the source plane and compute the flux and the amplification factor for an element area on the surface of the source. Then we integrate the amplified (or reduced) flux over the region of the source plane which is mapped within the image contour under consideration. Even though the surface brightness is invariant under gravitational imaging, the area of the source and hence the net flux we receive will generally not be conserved. We find that the excess flux (above the background) within the closed image contour produced by a source region whose angular coordinate has a constant x-component equal to α and a brightness distribution given by equation (10) is approximately

$$\Delta S = \pi a\theta_0^2[(\alpha^2 + 4\theta_0^2)^{1/2} - \alpha]\,\frac{B_0}{\Omega} . \tag{13}$$

Here a is a constant which depends on the detailed shape of the image contour, and $a \approx \frac{1}{4}$ for a typical contour having roughly the shape of a semicircle (cf. Fig. 2).

The average surface brightness contrast for an interior region is the ratio of this excess flux to the area enclosed by the image contour. If the physical area of the lens is small compared with the radius of the cone of inversion, we could in principle detect a point image very near the lens due to a distant bright region, and thus infer the presence of the deflector. However, the observations will be limited by finite resolution, and the average brightness over a typical region with angular resolution δ is

$$\Delta B \approx \frac{\Delta S}{\pi\delta^2} \approx \frac{a\theta_0^2[(\alpha^2 + 4\theta_0^2)^{1/2} - \alpha]B_0}{\Omega\delta^2} \tag{14}$$

for $\delta \ll \theta_0$. (The brightness contrast rapidly approaches zero as δ approaches θ_0.) If we choose the limiting contour so that $\alpha \approx \theta_0^2/\delta$, then the brightness contrast is approximately $\Delta B \approx 2aB_0\,\theta_0^2/\Omega\delta$. The criterion for significant contrast is therefore

$$\frac{\theta_0^2}{\Omega\delta} \gtrsim 1 \tag{15}$$

for interior image contours. It will always be satisfied if the angular resolution of the telescope is sufficiently high, in contrast to the criterion (12) for exterior contours which have a maximum brightness contrast for a given lens system. A test for discovering an interior gravitational lens image would be a surface brightness which increases according to equation (14) as the telescope resolution changes.

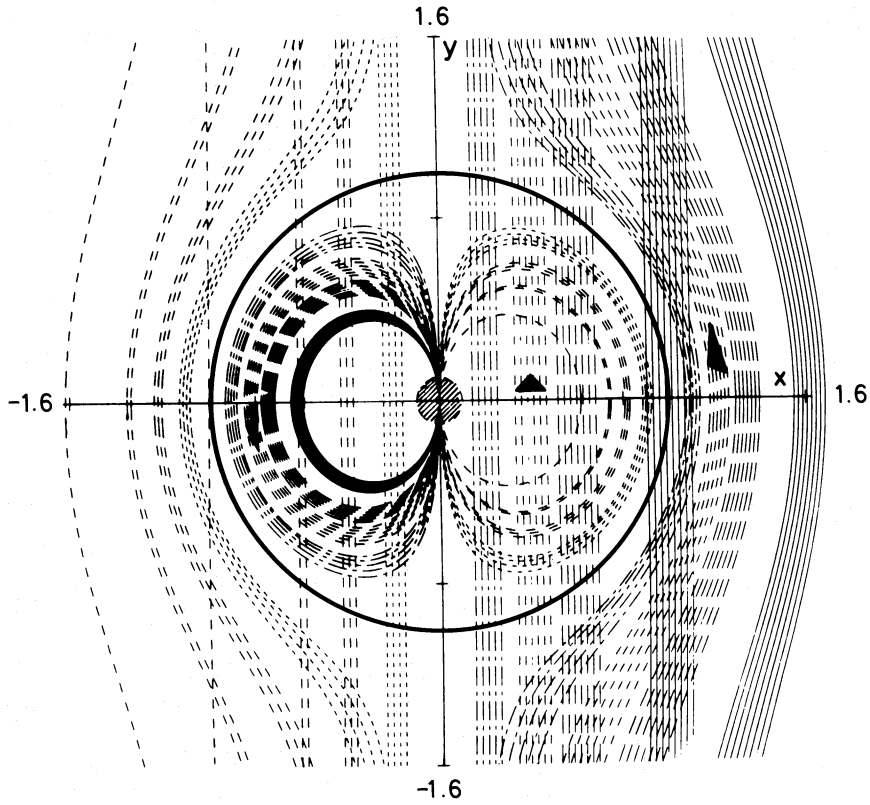

FIG. 2.—An array of straight-line source isophotes and their computed gravitational images

IV. EXAMPLES OF GRAVITY RINGS

We now examine the form of gravity rings which arise for a variety of source backgrounds, to illustrate the nature of the effect. Of course, in an astronomical observation one does not independently know the detailed form of the brightness distribution of the source. Fortunately, we shall see that many source structures lead to the same basic gravity ring effect.

Equation (5) may be used directly to obtain the shape of the image isophotes corresponding to a given source isophote. The Cartesian components of equation (5) give

$$x_I\left(1-\frac{\mu}{x_I^2+y_I^2}\right)=x \tag{16}$$

and

$$y_I\left(1-\frac{\mu}{x_I^2+y_I^2}\right)=y\,. \tag{17}$$

The source isophotes are given by the brightness $B(x, y)$ = constant. Substituting this in equation (16) or equation (17) to eliminate either x or y, and then eliminating the remaining source coordinate from the resulting pair (16) and (17), gives the image isophotes $y_I(x_I, \mu)$, provided that there are no singularities.

As a simple example, suppose that the source brightness varies linearly with distance x measured from the deflector (in asymptotically flat space):

$$B=B_0\left(1+\frac{x}{\chi}\right), \tag{18}$$

analogous to equation (10), with χ the linear scale length. Source isophotes therefore are given by particular values of x, and equation (16) gives the corresponding image isophotes $y_I(x_I, \mu, x)$. Examination of equation (16) immediately shows that for a given strength μ of the deflector and for the source isophote specified by x, the image isophotes are closed contours near the deflector within the circle of linear radius $\sqrt{\mu}$. Outside this radius they are extended distorted contours. Figure 2 illustrates this result. It shows an array of straight-line source isophotes, distinguished by their thickness and form of shading, being distorted by the central deflector, shown as a shaded disk. The solid-line circle denotes the cone of inversion, whose angular radius θ_0 sets the scale of the diagram. The distorted exterior images of the straight-line contours are open and lie entirely outside the cone of inversion on the same side of the lens as their source contours. The interior images are all closed and contained wholly within the cone of inversion, but are on the opposite side of the deflector from the exterior contours. The filled triangles (one of which is barely visible in the second interior contour on the left) indicate the sense of direction in the source and its corresponding image contours. Note that an interior image contour is oppositely directed to its exterior contour.

Figure 3 illustrates a somewhat more complicated example, where the source isophotes are groups of concentric circles positioned to one side of the deflector. Now the exterior images are displaced and distorted circles outside the cone of inversion (again represented by the solid circle around the deflector). The interior inverted images are closed curves within the cone of inversion but are on the other side of the lens from the exterior image if the source contour does not encompass the lens. (The

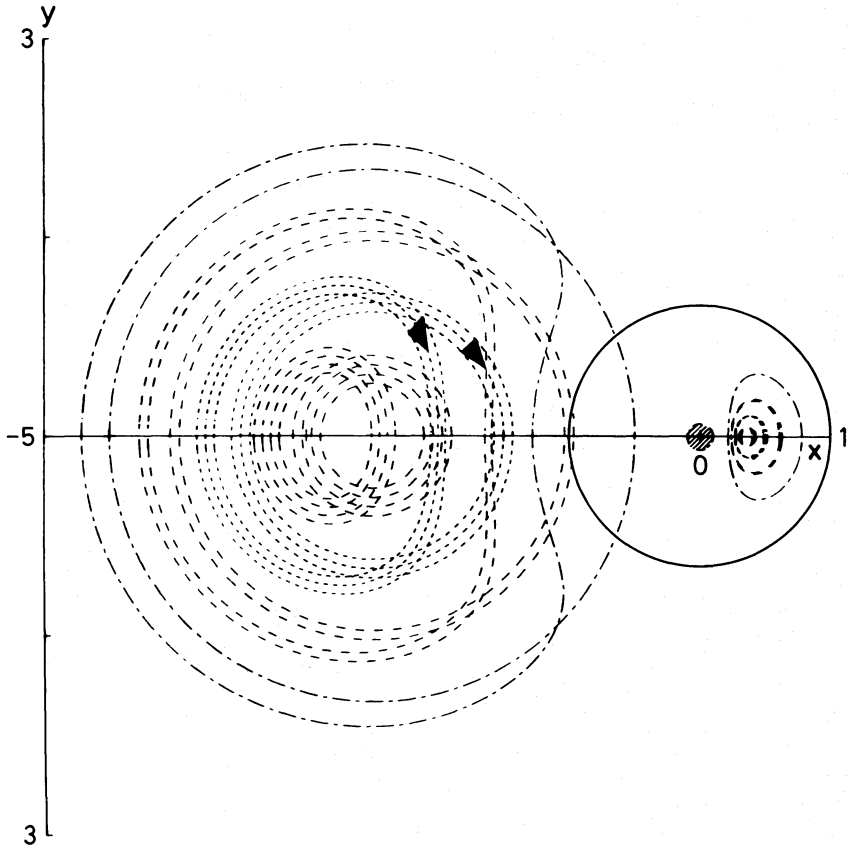

FIG. 3.—Concentric source isophotes imaged by an off-axis deflector

computer graphics could not quite cope with closing the innermost contour in this figure.)

In realistic astronomical observations, it is unlikely that the source isophotes will have any simple geometry. We are therefore interested in how the deflector changes the *texture* of the complicated isophotes of a given source. This aspect of the problem is most easily examined by constructing a gravitational analog lens, such as Liebes (1969) and Icke (1980) describe. Our lens is made of Plexiglas with a value of the strength parameter $R \equiv 4GM/c^2 = 0.5$ cm, an inner radius $r_1 = 0.63$ cm, and an outer radius $r_2 = 5.6$ cm. Its effective gravitational mass is 1.6×10^{27} g, about one-fourth the mass of the Earth. (It was simplest to turn the lens on a lathe, producing small ridges which give parts of the image a slightly ragged edge but do not affect the qualitative features we wish to illustrate.)

Figures 4–7 show the result of imaging a variety of background brightness textures. In each case we first show the undisturbed background, then the background distorted by a lens placed either 10 cm or 24 cm from the source. In each case the distance from the source to the focal plane is 68 cm and the photographs are taken through a 50 mm lens. Figure 4 shows images of isophotes parallel to the y-axis, as in Figure 2. The images using the Plexiglas lens agree with those calculated in the manner of Figure 2. Figure 5 shows images of a homogeneously textured pattern of nearly point sources. The images are essentially independent of the source pattern, as long as the separation of sources is much less than the cone of inversion. Figure 6 shows a meandering isophote and its images. Again the critical property is the average angular spacing of adjacent meanders relative to the cone of inversion. Details of the meanders count for little in the formation of the gravity ring around the cone of inversion. Finally, Figure 7 shows the results for a rather arbitrary arrangement of segmented linear isophotes.

From all these examples, we conclude that gravity rings will be robust and dominant features of sufficiently high-resolution observations of an extended background source of varying brightness imaged by a point (or nearly point) mass. The chief requirement is that the angular scale length of the background brightness variation be smaller than the cone of inversion.

V. DIAGNOSTIC USES OF GRAVITY RINGS

Once the importance and ubiquity of gravity rings are recognized, astronomical applications come readily to mind. We describe several in this section; undoubtedly the reader can think of more. The basis of most applications is the observed angular size of the ring structures, i.e., the cone of inversion. From equations (3) and (4), we see that knowledge of any two of the three parameters—deflector mass, observer-deflector distance, observer-source distance—enables the third to be determined. Moreover, if $l_{OD} \ll l_{OS}$, then the ring's angular radius depends on just M and l_{OD}, so independent knowledge of one of these quantities determines the other. Some representative applications are the following:

1. Determination of pulsar masses. Suppose that a pulsar produces a gravity ring image of a background radio cloud in our Galaxy, and we know the distance to the pulsar from its dispersion measure. If the cloud is at several times the distance of the pulsar, then we do not need its actual distance to obtain a fairly accurate estimate of the pulsar mass. If the background

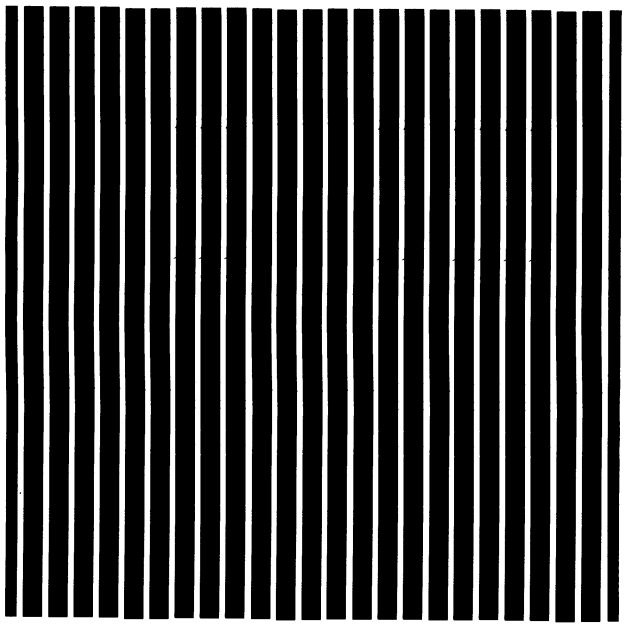

FIG. 4*a*

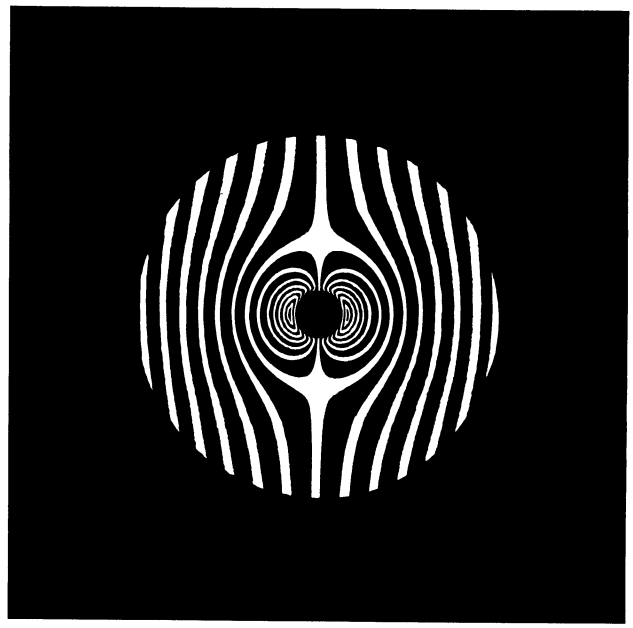

FIG. 4*b*

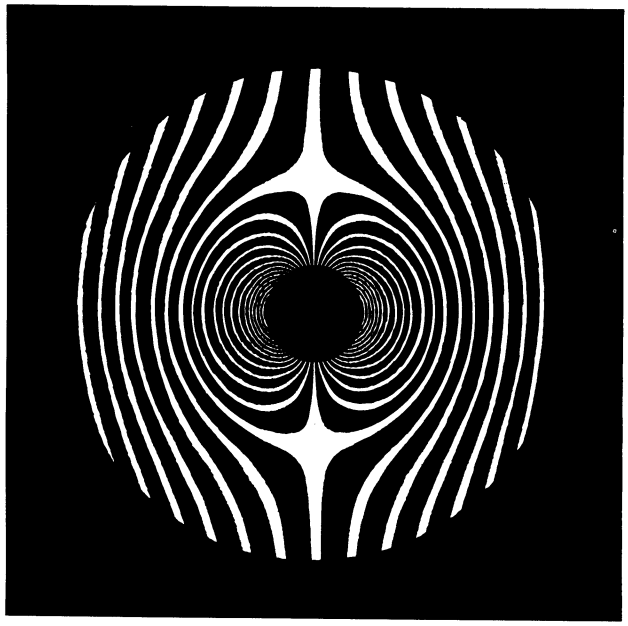

FIG. 4*c*

FIG. 4.—Images of thick parallel isophotes through a Plexiglas gravitational lens: (*a*) the undistorted isophotes; (*b*) $l_{DS} = 10$ cm; (*c*) $l_{DS} = 24$ cm. In all cases $l_{OS} = 68$ cm.

cloud's distance is of the same order as that of the pulsar, we may be able to estimate its distance from the galactic rotation law. Alternatively, if the cloud contains maser sources, it may be possible to find its distance quite accurately from the proper motions of these sources (Genzel *et al.* 1981) or by other means. Thus pulsar masses could be measured quite readily from the diameter of their gravity rings. It is also possible to independently measure the total mass of a binary pulsar this way (since for representative values its angular radius would be much less than θ_0). Since orbital parameters give the mass ratio, we could determine the masses of each component. Of course, this would apply to any binary system whose distance is known from independent measurements. In particular, high values of M might indicate a black hole component.

2. Detection of black holes or other dark compact objects by the gravity rings produced in background galactic emission. Since the deflector is always at the center of the ring, we can either identify it unambiguously or determine an upper limit to its apparent luminosity. We may be able to find its distance by the method described in item 9 below. Although the random probability of finding such an object in a VLBI map is small, we should be alert to its chance occurrence.

3. Determination of the relative mass spectrum of a cluster of stars which form gravity rings against a background cloud. The only variable in this configuration is the mass of the deflector. Independent determination of the distances of the cluster and cloud (if it is fairly close) would give the absolute mass spectrum.

4. Accurate masses for nearby stars whose distances are well known from their parallaxes.

5. Measuring the distance to a star or background cloud. If the deflector mass is known, we can find the distance to the deflector if the cloud is known to be much farther away. Even if the deflector mass is not known, it is possible to determine the relative distances of background clouds along the line of sight. The trick is to observe the different clouds at different frequencies where one or another cloud dominates. This would be easier if the emission comes from narrow maser lines than if it comes from broad molecular lines or the continuum. The fortunate case where a deflector of known mass and distance produces a gravity ring from a background planetary nebula or supernova remnant would be especially useful.

6. Detection of subresolution structure in background clouds. The basic condition for finding a gravity ring is that the cloud have luminosity contrast over scales much less than θ_0. The angular thickness of the ring produced by a spot of high density contrast in the source cloud is approximately the

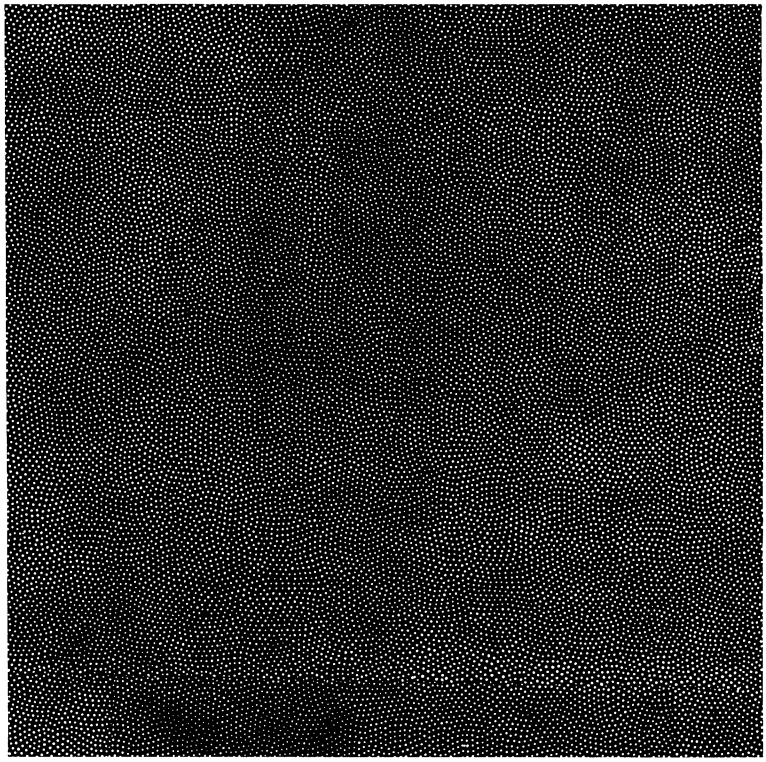

FIG. 5*a*

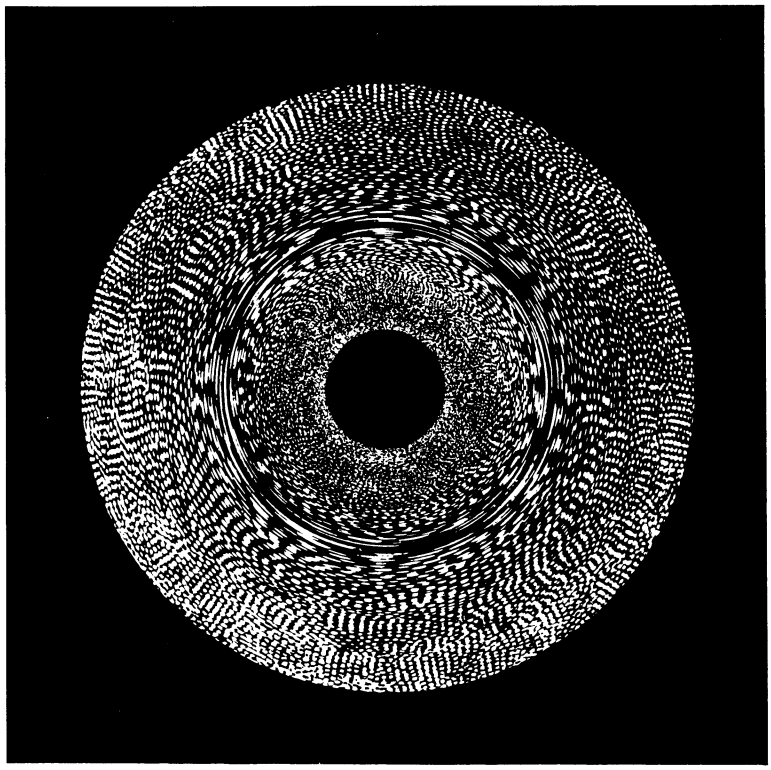

FIG. 5*b*

FIG. 5.—Images of a pattern of nearly point sources through a Plexiglas gravitational lens: (*a*) the undistorted isophotes; (*b*) $l_{DS} = 24$ cm. In both cases $l_{OS} = 68$ cm.

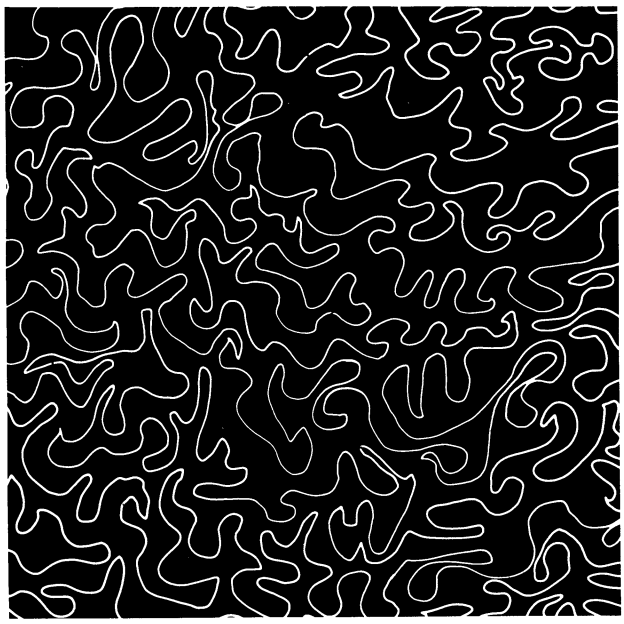

FIG. 6a

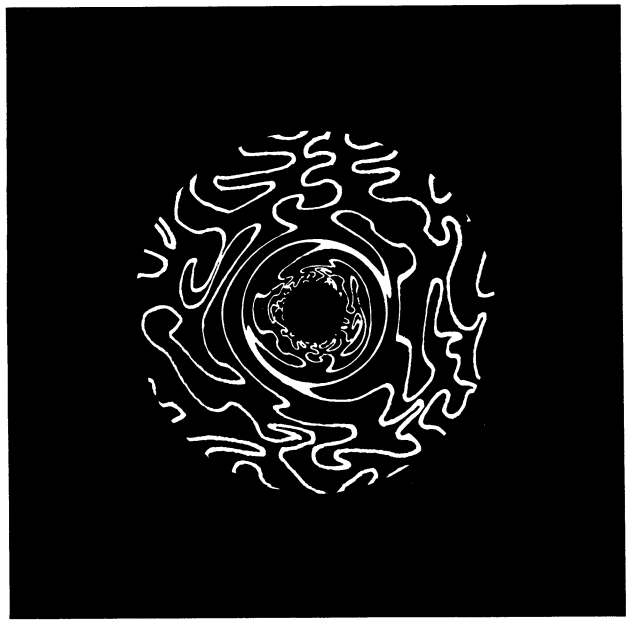

FIG. 6b

FIG. 6.—Images of a meandering isophote source through a Plexiglas gravitational lens: (*a*) the undistorted isophotes; (*b*) $l_{DS} = 10$ cm. In both cases $l_{OS} = 68$ cm.

angular diameter of the spot. Although a telescope may not be able to resolve the spot or the thickness of the ring directly, it may be able to establish the mere existence of the ring's large-scale pattern, and thus establish that the source is mottled on a smaller scale. The sudden appearance of a ring in a previously homogeneous source, for example, might indicate the onset of subcondensation and star formation. Another useful example would be detection of a steep intensity spike in the nucleus of our Galaxy, perhaps produced by an accreting black hole or other violent event there. This might show up as a gravity ring, even though it is too small to be resolved by itself.

7. Information from the absence of gravity rings. If gravity rings were not found on background clouds, it would be possible to put lower limits on the scale, and upper limits on the brightness contrast, of inhomogeneities in the region of the cloud imaged by the deflector. This would be especially interesting around the nucleus of our Galaxy.

8. Extragalactic information. Along lines of sight at fre-

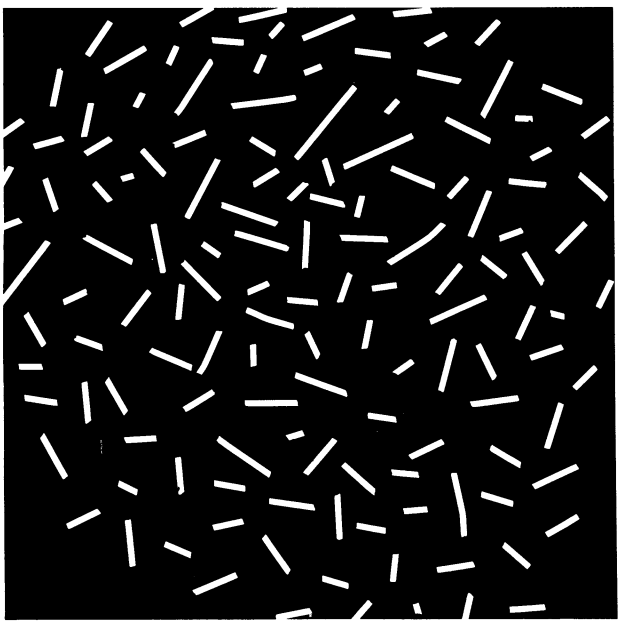

FIG. 7a

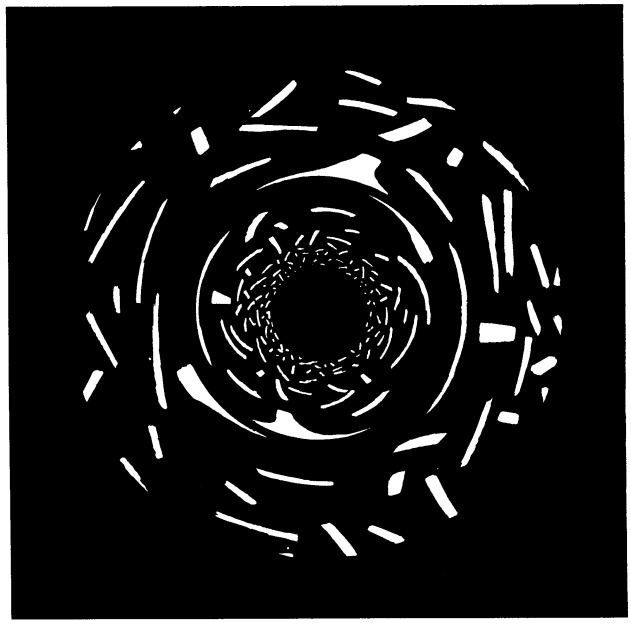

FIG. 7b

FIG. 7.—Images of an arbitrary arrangement of segmented linear isophotes through a Plexiglas gravitational lens: (*a*) the undistorted isophotes; (*b*) $l_{DS} = 24$ cm. In both cases $l_{OS} = 68$ cm.

quencies where there is no galactic background emission (at least to the level at which it is possible to establish this independently), it may be possible to use the presence or absence of gravity rings to learn about the homogeneity of extragalactic radiation, including the microwave background. Nuclei of radiogalaxies, or hot spots in their extended lobes, may also be imaged by an object in our Galaxy.

9. Time variations of gravity rings. These changes also carry much significant information. Part of the variation will be caused by the Earth's paralax, and can be recognized by its periodicity. As the background cloud is positioned differently with respect to the deflector along the line of sight, the apparent pattern changes. The amount of this change may make it possible to find the distance of the deflector (and possibly its mass). Time variations will also arise from proper motion of the deflector and the source (to a lesser extent when it is much more distant) and from intrinsic changes in the source.

10. Transverse velocity measurement. This is a basic problem of astronomy. If the transverse motion of the deflector is sufficiently high, it will alter the appearance of the gravity ring on a time scale shorter than $\tau \approx \theta_0 l_{OD}/V_{\text{transverse}}$. One indication that a change is caused by transverse deflector motion rather than by an intrinsic evolution of the source is that it occurs simultaneously at all frequencies. Observations of these changes may enable $V_{\text{transverse}}$ to be estimated.

It is clear from our analysis that the use of gravity rings will make it possible to measure fundamental properties of an increased range of astronomical objects with considerable accuracy.

W. C. S. is happy to thank Cambridge-Bombay Society and the Tate Institute for Fundamental Research for their generous hospitality during his 1983 November–1984 January visit. It is also a pleasure to thank Dr. P. K. Kunte for fabricating the gravitational lens and Mr. Richard Sword for his very skillful photography through this eye of gravity.

REFERENCES

Barnothy, J. M. 1965, *A.J.*, **70**, 666.
Bontz, R. J. 1979, *Ap. J.*, **233**, 402.
Bourassa, R. R., and Kantowski, R. 1975, *Ap. J.*, **195**, 13.
Einstein, A. 1936, *Science*, **84**, 506.
Genzel, R., Ried, M. J., Moran, J. M., and Downes, D. 1981, *Ap. J.*, **244**, 884.
Gott, J. R. 1981, *Ap. J.*, **243**, 140.
Icke, V. 1980, *Am. J. Phys.*, **48**, 883.
Liebes, S. 1964, *Phys. Rev. B*, **133**, 835.
———. 1969, *Am. J. Phys.*, **37**, 103.
Narasimha, D., Subramanian, K., and Chitre, S. M. 1982, *M.N.R.A.S.*, **200**, 941.
Refsdal, S. 1964, *M.N.R.A.S.*, **128**, 295.
Stockton, A. 1980, *Ap. J. (Letters)*, **242**, L141.
Walsh, D., Carswell, R. F., and Weymann, R. J. 1979, *Nature*, **279**, 381.
Young, P., Gunn, J. E., Kristian, J., Oke, J. B., and Westphal, J. A. 1981, *Ap. J.*, **244**, 736.
Zwicky, F. 1937, *Phys. Rev. Letters*, **51**, 290, 679.

S. M. CHITRE: Tata Institute of Fundamental Research, Homi Bhabba Road, Bombay 400 005, India

D. NARASIMHA: Department of Physics, University of Calgary, 2500 University Drive NW, Calgary, Alberta, Canada T2N 1N4

WILLIAM C. SASLAW: Astronomy Department, University of Virginia, P.O. Box 3818, University Station, Charlottesville, VA 22903-0818